Bond calculation of optical second-harmonic generation at gallium- and arsenic-terminated Si(111) surfaces

1992 J. Phys.: Condens. Matter 4 4017

(http://iopscience.iop.org/0953-8984/4/15/015)

J. Phys.: Condens. Matter 4 (1992) 4017–4037. Printed in the UK

Bond calculation of optical second-harmonic generation at gallium- and arsenic-terminated Si(111) surfaces

C H Patterson, D Weaire and J F McGilp

Department of Pure and Applied Physics, University of Dublin, Trinity College, Dublin 2, Ireland

Received 17 December 1991

Abstract. An *ab initio* valence bond method based on finite-sized clusters is proposed for calculating the non-linear electric susceptibilities of covalent solids, particularly those that are directly related to their efficiency for second-harmonic generation. It is presented as a radical alternative to electronic band-structure methods for these dielectric response functions and it is applied here to two Si surfaces. In its present form it is limited to the response to static fields. Linear and non-linear parts of the electric susceptibility are obtained from generalized valence bond calculations on clusters representing gallium- and arsenic-terminated (1 x 1) Si(111) surfaces. In the valence bond model for these covalent systems the self-consistent orbitals are localized in bond pairs and lone pairs. Electric susceptibilities are constructed by summing bond polarizabilities or hyperpolarizabilities of electron pairs in the surface layer. The major sources of non-linear polarization in the cluster lie along bond axes; hence optical second-harmonic generation at a covalently bonded surface may depend strongly on the surface structure. An additional major source of non-linear polarization exists perpendicular to the axes of bent bonds which becomes dominant when the bond is severely bent. Calculated non-linear susceptibilities are in good agreement with absolute measurements of second-harmonic generation intensity.

1. Introduction

In the early 1970s, Levine [1] developed a phenomenological bond charge model for calculating non-linear susceptibilities of covalent and polar–covalent solids. This involved analytic expressions for bond non-linearity in terms of differences in covalent radii and ionicity of the bonded pair of atoms, and the average band gap of the material. Levine's method proved very successful in quantitatively predicting non-linear susceptibilities and in explaining trends in susceptibility as a function of ionicity etc. Around the same time, Jha and Bloembergen [2] and Flytzanis and Ducuing [3] calculated the low-frequency limits of non-linear susceptibilities of III–V compounds using tetrahedral bond orbital models. There were also early calculations, based on electronic band-structure techniques, by Aspnes [4] and Fong and Shen [5], and these techniques are still being used. However, when band-structure techniques are applied to materials with primitive unit cells much larger than that of diamond, there are difficulties in identifying the sources of non-linear polarization in the solid: there are also enormous demands on computer time. The calculation, when formulated in terms of perturbation theory and band-structure, expands rapidly with the size of the system and is not practicable for many systems for which a theoretical calculation of the non-linear susceptibility is highly desirable. This is illustrated by a recent pioneering

0953-8984/92/154017+21$04.50

calculation of second-harmonic generation in odd-period Si_nGe_n superlattices and at the SiGe interface [6]. For the superlattice material, Si_5Ge_5, the calculation required 90 hours of supercomputer time [6]. A method is therefore sought that is fundamental, computationally inexpensive and will readily yield a simple model for sources of non-linear polarization in the solid. The work cited may provide a clue to development of such a model, in as much as the results were seen to be consistent with additive bond contributions [6]. A return to the bond model is thereby suggested.

In the method to be presented below, non-linear susceptibility matrices derived from bond hyperpolarizabilities are calculated, without adjustment of parameters, for gallium- and arsenic-terminated (1 × 1) Si(111) surfaces. These matrices describe the response of the surface charge density to electric fields, and their calculation is central to understanding the optical response at surfaces and interfaces. Linear and non-linear polarizabilities are obtained by applying electric fields to clusters (figure 1) which represent the surfaces, and calculating the polarization of localized bond orbitals as a function of applied field strength. The calculation is formulated in terms of responses of electron pairs (bond pairs and lone pairs) which are summed over the unit cell to give the total response.

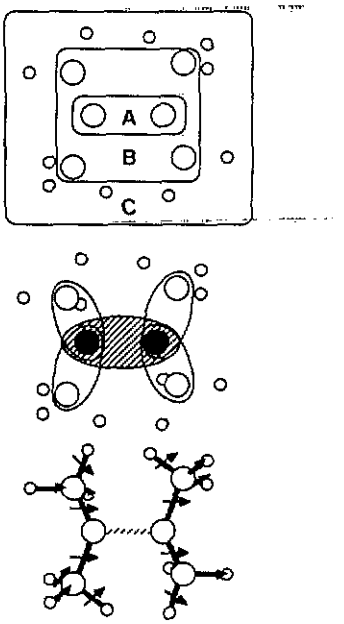

Figure 1. Schematic representation of a cluster calculation. Top: cluster of atoms used to calculate response properties of the bond between the two atoms in region A. The next shell of atoms, B, provides an electronic environment for the bond in A which represents the remainder of the surface or bulk of the solid being modelled. The final shell, C, is an artificial termination by pseudo-hydrogen atoms. Middle: the valence bond model naturally yields occupied bond orbitals localized on all bonds. Bottom: the change in the electric field at the bond in region A from dipoles induced in surrounding bonds, together with the externally applied field, constitute the local field at the bond in region A. This field is computed, *ab initio*, at points along the A bond axis. This allows the response of the bond in region A, calculated by applying a field to the cluster, to be corrected for effects of interaction with other bonds.

Long-range (dipolar) interactions between polarized bonds cannot be neglected in summing responses of bonds to an applied field. Thus there is no simple additivity of bond polarizability and hyperpolarizability that would yield the overall linear and non-linear responses of the solid. A particular bond is polarized by the applied field together with the field arising from dipoles induced within the solid or at the surface. The combination of these fields is the local field which is discussed in more detail below. A static field is applied in a self-consistent-field (SCF) cluster calculation which polarizes bonds in the cluster (figure 1). Induced dipolar fields are present in the SCF charge density. However, these fields are specific to the particular cluster and differ

from the fields in a macroscopic surface. It is therefore necessary to obtain bond parameters for bonds that are *independent* of the surrounding bonds, in order that cluster calculations may give results which are transferable to macroscopic surfaces or bulk solids. These are obtained by computing the local field acting on a particular bond and fitting the bond parameters from the bond response to the local field. The response of a macroscopic surface or bulk solid to an applied field is obtained in a second calculation of the polarization using these independent bonds coupled by dipolar fields. Independent bond parameters are termed 'bare' while parameters fitted using only the applied field are termed 'dressed'. In certain respects, the approach developed here is similar to the interacting segment model (ISM) of Miller, Orr and Ward [7]. In the ISM, electrostatic interaction between adjacent segments of a molecule is taken into account and this was shown to give substantial improvement over simple bond additivity as a basis for understanding electric tensor properties of chlorofluorocarbon molecules.

Within the valence bond model of electronic structure for molecules and solids, bond types may be classified according to the number of spin-paired orbitals localized between a pair of bonded nuclei, and their shapes. In solids, bonds are usually single bonds, there being only a single pair of spin-paired orbitals localized between the nuclei, but in molecular systems, especially carbon molecules, there are commonly double and triple bonds with four or six localized orbitals spin-paired into two- or three-bent-bond arrangements [8]. If the shapes of these orbitals are compared between one molecule and another containing, according to this simple analysis, the same type of bond, a remarkable degree of similarity is usually found in the shapes of the localized valence bond orbitals [9, 10]. However, the possible change in the polarizability and hyperpolarizability for two bond pairs of the same type in similar, but not identical, electronic environments is as yet unknown. For example, Si–Si bonds occur both in bulk Si and Si–Ge superlattices, but without performing calculations on clusters representing both of these, it is impossible to say whether there will be a marked difference between the independent bond parameters determined for the Si–Si bond in bulk Si compared to the same bond type in the Si–Ge superlattice, due to different surrounding bonds (Si–Si, Si–Ge and Ge–Ge versus only Si–Si). At this stage we use the similarity in shapes of orbitals in the strong fields of nuclei and neighbouring electron pairs in different molecules as a plausibility argument that bond responses in relatively weak externally applied fields should also be similar. A calculation of linear and non-linear bond polarizabilities, which contribute independently (apart from the interaction mentioned above) to the optical properties of a bulk solid or surface, is therefore envisaged.

While the derived bond parameters can be applied to a number of response properties of bulk solids and their surfaces, the emphasis here is on calculating the (non-resonant) optical second-harmonic response. Optical second-harmonic generation (SHG) is still in its early stages of development as a technique for studying surfaces and interfaces [11–14]. Its surface and interface sensitivity arises because the bulk second-order response is zero in a centrosymmetric medium within the dipole approximation. For a material such as crystalline silicon, the surface can dominate the second-harmonic response at certain excitation frequencies [11]. Generally, surface SHG experiments are carried out with incident photon energies in the range 1 to 3 eV, where the excitation or second-harmonic fields may cause direct transitions between surface and interface states and therefore, resonant behaviour, producing a strong variation in optical properties.

The specific connection between bond polarizabilities and second-harmonic generation is as follows: the second-harmonic intensity depends on the square of the second-order polarization in the solid, $P_i^{(2)}$. The total polarization, P_i, per unit volume (equation (1)) is usually expressed as a polynomial series in the applied field strength, $\boldsymbol{E}$, where the susceptibility coefficients are independent of field strength but will, in general, depend on the frequency of the applied field:

$$P_i = \epsilon_0 \left(\chi_{ij}^{(1)} E_j + \chi_{ijk}^{(2)} E_j E_k + \ldots \right) \tag{1}$$

where ϵ_0 is the vacuum permittivity and $\chi^{(m)}$ is the susceptibility at mth order in field strength. So the second-harmonic intensity depends on $\chi_{ijk}^{(2)} E_j E_k$. In sections following we show how $\chi_{ijk}^{(2)}$ may be obtained as a sum over second-order bond polarizabilities.

2. Structures

Calculations are presented for two Si(111) surfaces, terminated in a 1×1 surface unit cell either by As or Ga. The major motivation for studying the optical properties of these surfaces theoretically was that parallel, experimental SHG and surface Raman studies have been performed in this laboratory [15] and elsewhere [16] and a tight-binding band-structure calculation for the second-harmonic response of As-terminated Si(111) was also in progress [17]. The As-terminated surface was initially studied by Uhrberg *et al* [18], who measured the surface band-structure and calculated the surface states. Since then this surface has been extensively studied by theoretical [17–21] and experimental [18, 22, 23] methods. The structure of the surface is known from x-ray standing wave [22] and medium-energy ion scattering experiments [23]: the As atoms that replace the last layer of Si atoms are relaxed 0.22 Å outwards from the bulk-terminated Si(111) positions. Theoretical calculations for the surface structure based on periodic boundary conditions [18] and cluster techniques [20] are in good agreement with the experimentally determined structure. The 1×1 Ga-terminated surface has not been so thoroughly studied. Its surface structure has been studied experimentally by LEED [24], the x-ray standing wave technique [24] and scanning tunnelling microscopy [25] and the surface structure has been calculated by a density functional technique [24]. LEED studies indicate that there may be weakly bound Ga present in a Ga monolayer on Si(111) [24], in addition to the Ga bonded in the substitutional sites (which are equivalent to those occupied by As) *or* the '1×1' surface may relieve strain by incorporating an ordered missing Ga defect structure [24]. The surface structure determined by x-ray standing waves has the substitutional Ga atoms 0.50 ± 0.02 Å below the bulk-terminated Si(111) positions, and this large inwards relaxation of the Ga atom agrees with the Si–Ga bond length of 2.23 Å [24] calculated by the density functional technique, which is 9% smaller than the sum of the covalent radii and corresponds to an inwards relaxation of 0.59 Å. An inward relaxation of 0.16 Å (corresponding to a Si–Ga bond length of 2.30 Å, 6% shorter than the sum of covalent radii) was obtained by us in a cluster calculation of the minimum energy position for Ga in the 1×1 substitutional site, identical in methodology to a previous calculation of the equilibrium position of As in the same site [20]. Calculations described below were performed with the As or Ga atoms at their equilibrium computed bond lengths.

3. Application of cluster calculations to response properties

In this section the difficulties inherent in using clusters to model optical properties of solids are discussed. In particular, attention is given to how the edges of clusters are treated, why the localized orbitals of a generalized valence bond (GVB) wave function make it especially suitable for cluster modelling of optical properties, and how the local field mentioned above is to be calculated.

Cluster techniques have been successful in predicting surface [20, 26] and bulk defect [27–29] structures and they have been used to interpret chemical bonding in these structures [20, 26, 27]. Wave functions based on valence bond, Hartree–Fock (HF), density functional techniques etc are computed for a cluster chosen to represent a particular system, which must be terminated appropriately [27]. In making the assumption that, for example, a macroscopic surface can be adequately represented by a small cluster of atoms, the ground state charge density is implicitly assumed to be largely determined by the *local* configuration of atoms. This is expected to be a very good approximation for metals since any static, external perturbation is screened by the valence electrons over short distances; in a semiconductor the approximation is not expected to be as good. However, cluster modelling of covalently bonded materials by valence bond methods is simpler than for metals because the valence orbitals of the covalent material localize in well-defined bond regions. Covalent clusters can therefore be terminated economically in an obvious way, using hydrogen-like atoms. Such cluster-terminating atoms are used in this work: they preserve charge neutrality of silicon atoms to which they are bonded [26, 27].

The second important consideration is concerned with the functional form of cluster wave function (GVB, HF etc). A wave function that facilitates partitioning of the charge density into 'representative' and 'terminating' parts is required, the former referring to those parts of the charge density that are to be identified with parts of the unit cell being modelled, and the latter to those that belong to the terminating-atom bonds. The GVB wave function [30] provides such a separation since the orbitals of this wave function are localized. It has the form

$$\Psi_{\mathrm{GVB}} = A\left[\phi_{1\mathrm{A}}\phi_{1\mathrm{B}}\phi_{2\mathrm{A}}\phi_{2\mathrm{B}}\cdots\phi_{N\mathrm{A}}\phi_{N\mathrm{B}}\right]\Theta \tag{2}$$

where A is the antisymmetrization operator, $\phi_{1\mathrm{A}}$ and $\phi_{1\mathrm{B}}$ are a pair of overlapping, singly occupied orbitals and Θ is the spin function which is a sum of spin eigenfunctions. In principle, all GVB orbitals may overlap to an extent determined in the self-consistency process, and Θ is a complete set of spin eigenfunctions. This wave function is computationally complex but considerable simplification can be obtained by introducing the strong orthogonality and perfect pairing approximations [30], in which electron pairs are constrained to be orthogonal to one another and only the perfect pairing spin eigenfunction, Θ_{pp}, with the form

$$\Theta_{\mathrm{pp}} = (\alpha\beta - \beta\alpha)(\alpha\beta - \beta\alpha)(\alpha\beta - \beta\alpha)\ldots \tag{3}$$

is retained. A more extensive description of this wave function, and its relationship to others incorporating electron correlation effects and the HF wave function, was given recently [10].

The orbitals of a GVB wave function partition the charge density into bonds *within* the representative part of the cluster and those *between* the representative part and

the terminating atoms. More exactly, it is impossible to separate the cluster response in the same way since, for example, the induced dipoles of each part interact strongly, as noted in section 1. Indeed it will be shown that the induced fields can be as large as the applied field. The local field that acts on the representative part of the cluster charge density is therefore unique to the cluster, but the total electric field at any point in the cluster can be computed and so can the local field at a bond arising from all other induced dipoles.

The local field acting at a given bond was defined as the applied field plus the induced field arising from polarization of all charges except the bond itself. This differs in its definition from the conventional 'local field effect' of semiconductor dielectric theory (appendix A). Induced fields vary on the scale of interatomic distances in the solid, but the simple approximation of weighting the induced field along a bond by the charge density of the bond orbital gives an *average local field* for the whole bond, when added to the applied field. 'Dressed' polarizabilities, $\alpha_{n,ij}$, and hyperpolarizabilities, $\beta_{n,ijk}$, $\gamma_{n,ijkl}$ (appendix B), for the nth bond pair are obtained by fitting induced dipoles in the bond orbitals p_n, to the expression

$$p_{n,i} = \epsilon_0 \left(\alpha_{n,ij} E_j + \beta_{n,ijk} E_j E_k + \ldots\right) \tag{4}$$

where E_j and E_k are components of the applied field, E. 'Bare' polarizabilities, $\alpha'_{n,ij}$, and hyperpolarizabilities, $\beta'_{n,ijk}$, $\gamma'_{n,ijkl}$, which have been corrected for induced fields in the cluster, are calculated (equation (4)) by fitting induced dipoles using the average local field, $\mathcal{E}$, rather than the applied field.

Having obtained such bare polarizabilities for the necessary bond types, they may be used to calculate the response of a macroscopic surface or bulk solid. In doing so we must again take account of the dipolar interactions. In a model of a macroscopic solid surface or bulk, a bare bond polarizability matrix (appendix B) is placed in the centre of each bond, the 'active site' of the ISM model. The local field resulting from the linear response at each of N bond sites is obtained by solving $3N$ linear equations which incorporate dipolar interactions between bond sites and give the induced dipole of the nth bond, p_n, in an applied field, E, which may be constant or varying in space (equation 5)

$$p_{n,i} = \alpha'_{n,ij} \left(E_j + \sum_{m \neq n}^{3N} \frac{1}{4\pi\epsilon_0} \frac{3(n_{mn} \cdot p_m) - p_{m,j}}{r_{mn}^3} \right) \tag{5}$$

where $\alpha'_{n,ij}$ is the bare polarizability matrix of the nth bond, n_{mn} is a unit vector from the mth bond directed towards the nth bond, r_{mn} is the distance between the mth and nth bonds and p_m is the dipole at the mth bond. These equations can be solved either for a large but finite cluster, or with periodic boundary conditions. Bare polarizabilities for the Si–Si bond, coupled via dipolar interactions as in (5) in the presence of a static, sinusoidal applied field with wave vector q, are currently being used to obtain the static dielectric constant of bulk silicon [31],

$$\lim_{q \longrightarrow 0} \frac{1}{\epsilon^{-1}(q', q; 0)}$$

in order to test the reliability of this approach to dielectric response in semiconductors. In this way the computation of the linear response is reduced to appropriate cluster

calculations followed by solution of a set of linear equations: if bond parameters prove to be reproducible from one solid to another for a particular bond type, then only the linear equations remain to be solved.

To obtain the non-linear response, hyperpolarizability matrices are placed at the bond sites and the local field from the linear response calculation is used to obtain the non-linear response. This assumes that the non-linear polarization from bare hyperpolarizability sources is small enough to be considered as a perturbation: otherwise a new set of equations incorporating hyperpolarizabilities might be solved by iteration. Single-cluster calculations for the systems studied here require about 15 minutes of computer workstation CPU time and a similar amount of time is required to solve the linear equations.

In the present paper, non-linear susceptibilities are obtained for macroscopic surface bilayers of the two surfaces studied by summing dressed hyperpolarizabilities in the surface unit cell. The local field is not taken into account in these susceptibilities. In a later paper the local field will be considered in the macroscopic non-linear response in the manner described above. Linear and non-linear bare bond matrices for these surfaces are reported here and used to analyse major sources of non-linear polarization in the surfaces.

4. Method of calculation

Calculations for the hydrogen molecule are first briefly described, which illustrate the method. Description of the method is then extended to clusters and calculation of local fields.

A hydrogen molecule is placed so that its bond axis is collinear with two remote charges of opposite sign so that it experiences a constant static field. The nuclei are held fixed at the equilibrium internuclear separation and the electronic wave function is computed in the presence of the field. This is repeated for several field strengths and the molecular dipole is also computed so that the polarization of the molecule is obtained as a function of field strength. The molecular polarization is then fitted to a polynomial in field strength whose coefficients are $\alpha_{ij}, \beta_{ijk}, \gamma_{ijkl}, \ldots$ (equation (4)). Note that the hydrogen molecule is centrosymmetric and $\beta = 0$. These polarizabilities and hyperpolarizabilities are given in table 1 for several basis sets. The other elements of the polarization matrices are calculated by placing the remote charges perpendicular to the bond axis. A trivial but instructive result for the first hyperpolarizability of a model system can be obtained by transferring a tenth of the hydrogen nuclear charge from one nucleus to the other, producing a 'hydrogen' molecule which is still neutral but now has one slightly more electronegative atom and one slightly less electronegative than a 'real' hydrogen atom. The first hyperpolarizability for this modified molecule parallel to the bond axis is non-zero since it is no longer centrosymmetric. The hyperpolarizability tensor for this molecule is given in table 2 for a single basis set. The first hyperpolarizability tensor for this system has *only two* unique, non-zero elements (appendix B). It will be shown that the second-order polarization of an independent, asymmetric bond in a cluster can also be described by a small number of elements whose physical interpretation is clear.

The local field acting on each bond orbital with an external field applied is calculated after the self-consistent calculation is completed. This is done by removing the bond orbitals of the bond in question from the converged total wave functions,

Table 1. Hartree–Fock static polarizabilities (α) and second hyperpolarizabilities (γ) for the hydrogen molecule[a].

Basis set [b]	$\alpha_{\parallel\parallel}$ (10^{30} m^3)	$\alpha_{\perp\perp}$ (10^{30} m^3)	$\gamma_{\parallel\parallel\parallel\parallel}$ (10^{51} m^5 V^{-1})	$\gamma_{\perp\perp\perp\perp}$ (10^{51} m^5 V^{-1})
2s	10.48			
2s1p	10.24			
4s2p	11.90			
4s2p2d		8.44		3.86
Extended [c]	11.90	8.53	4.84	4.00
Experiment	11.90[c]	8.53[c]	$\bar{\gamma} = 4.57$[d]	

[a] The z and x axes are parallel and perpendicular to the molecular axes, respectively. Some non-zero elements in the γ-tensor have not been calculated.
[b] Full basis set details are given in appendix B.
[c] The theoretical values were shown to have converged for these extended basis sets [47].
[d] $\bar{\gamma} = (8\gamma_{\perp\perp\perp\perp} + 12\gamma_{\perp\perp\parallel\parallel} + 3\gamma_{\parallel\parallel\parallel\parallel})/15$ [48].

Table 2. Hartree–Fock first hyperpolarizabilities (β), in units of 10^{-41} m^4 V^{-1} for a modified hydrogen molecule[a] using the 4s2p basis set.

	$\perp\perp$	$\perp'\perp'$	$\parallel\parallel$	$\perp'\parallel$	$\perp\parallel$	$\perp'\perp$
$\perp$	0.0	0.0	0.0	0.0	−0.4	0.0
$\perp'$	0.0	0.0	0.0	−0.4	0.0	0.0
$\parallel$	−0.4	−0.4	−1.6	0.0	0.0	0.0

[a] The molecule was modified by transferring 0.1 proton charge from one nucleus to the other along the positive $\parallel$ axis. $\perp$ and $\perp'$ refer to two orthogonal axes perpendicular to the bond axis.

with and without an applied field, then calculating the electric fields along the bond axes: the difference between these two fields is the induced field. As defined above, the local field acting at a point on the bond axis is the applied field plus the induced field. The average local field is taken as the mean of the induced field at ten points along the bond axis, weighted by the bond orbital charge density at those points. This field, $\mathcal{E}$, is then used to extract the bare bond matrices (equation (4)). Sometimes the averaged induced field strength is of similar magnitude to the applied field, *even in directions perpendicular to the applied field*, which emphasizes the importance of induced fields in describing how the bond charges interact when they are polarized.

5. Results

Two coordinate systems are used in the next section, surface and bond coordinates, illustrated in figure 2. Surface coordinates are appropriate for surface susceptibilities while bond coordinates are used for bond polarizabilities.

Self-consistent GVB wave functions were computed for clusters representing the Si(111) 1 × 1 As- and Ga-terminated surfaces, as illustrated in figures 3 and 4 by the cluster structures and valence bond orbitals for the Si–As and Si–Ga bond pairs and the As lone pair. These wave functions were successively computed for applied fields in the x, y, z, (x and y), (x and z), and (y and z) directions in surface coordinates; details of computations are given in appendix C. In order to have a non-linear

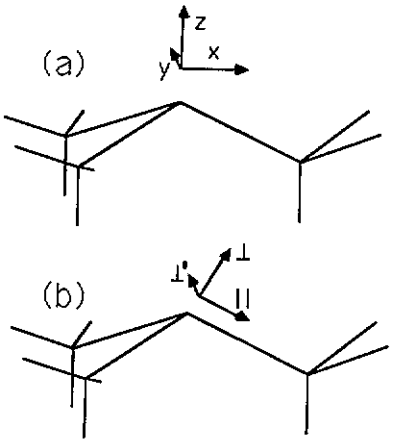

Figure 2. Diagram showing (*a*) surface coordinates for a whole cluster and (*b*) bond coordinates for a single Si–As or Si–Ga bond.

polarization large enough to be distinguished from numerical errors in computed polarizations, field strengths $\sim 10^8$ V m^{-1} were used, which are approximately ten times greater than typical experimental values [11]. Tests showed that the non-linear coefficients obtained were the same when a field strength ten times greater was employed. Dressed polarizability matrices obtained from this curve fitting are given in table 3. Note in particular that the bond matrices are not symmetric, so the bond response does not satisfy Onsager's principle [32], which requires that the bond polarizability matrices be symmetric:

$$\alpha_{n,ij} = \alpha_{n,ji}. \tag{6}$$

This principle is, of course, satisfied by the whole cluster but not, at this stage, individually by its component parts, the valence bond orbitals, since they interact strongly as they polarize in an applied field. The consequence of this for dressed bond parameters is that they are dependent on the environment and cannot be transferred from one solid to another or from cluster to solid. For the analysis that follows it is postulated that bond pairs, in their responses to applied fields, interact predominantly through the (classical) induced fields that they exert on one another, as they polarize in an applied field. This is reasonable for bond pairs, which must be in separate regions of space because of Pauli exclusion.

Table 3. Dressed polarizabilities for (*a*) Si–As and (*b*) Si–Ga bonds in bond coordinates, and (*c*) the As lone pair in surface coordinates, in units of 10^{-30} m^3.

(*a*)	⊥	⊥′	||	(*b*)	⊥	⊥′	||	(*c*)	*x*	*y*	*z*
⊥	6.4	0.0	1.4	⊥	5.8	0.0	−13.4	*x*	18.5	0.0	0.0
⊥′	0.0	8.9	0.0	⊥′	0.0	16.9	0.0	*y*	0.0	18.1	0.0
||	8.4	0.0	36.1	||	8.3	0.0	39.2	*z*	0.0	0.0	15.0

The induced field and bond charge density along the Si–As bond in the $Si_3AsH_9^x$ cluster (where H^x is a modified hydrogen atom; see appendix C) are shown in figure 5,

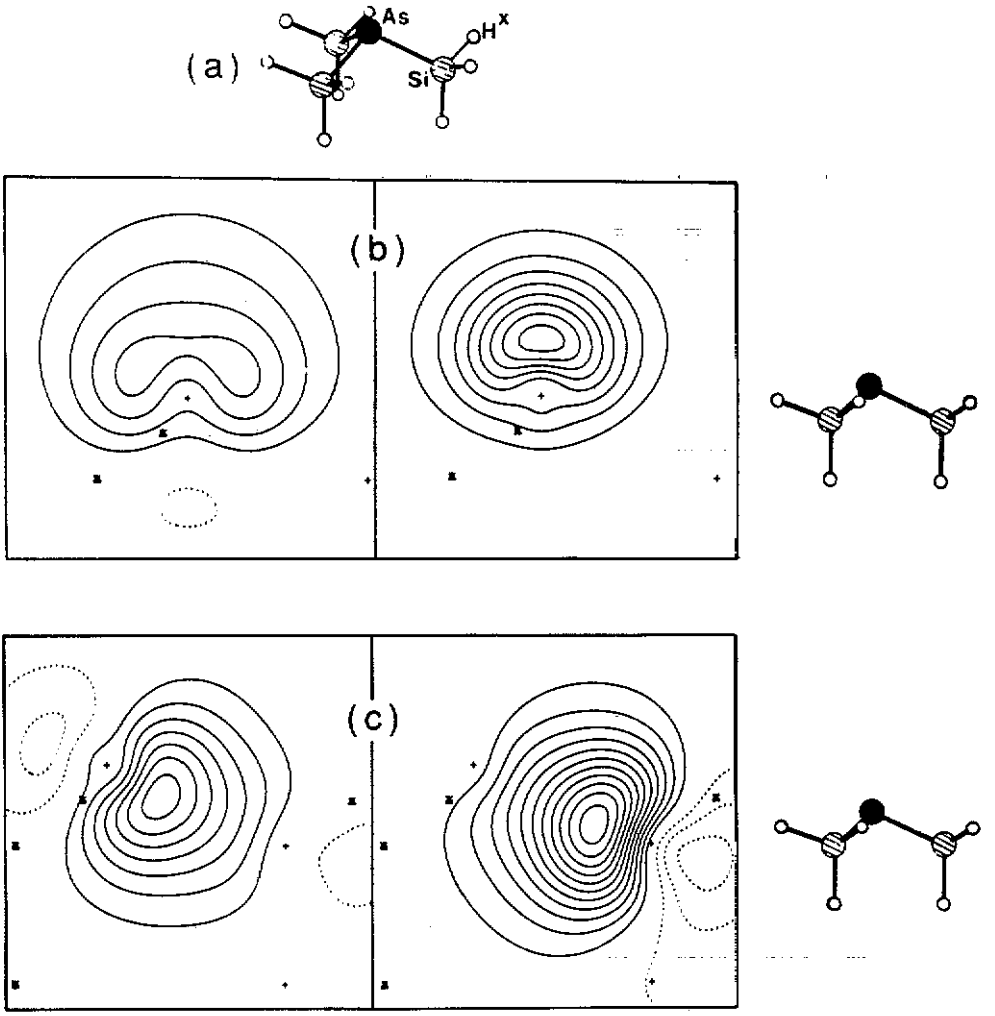

Figure 3. A schematic diagram (*a*) of the $Si_3AsH_3^x$ cluster and contour plots of (*b*) the As lone pair GVB orbitals and (*c*) the Si–As bond GVB orbitals. Contour intervals are 0.02 au. Crosses indicate atomic positions in the plane while triangles and X symbols indicate atomic positions in front of and behind the plane, respectively.

for a field applied in the x direction. Note that the induced field and the applied field are roughly equal in magnitude in the region where bond charge is concentrated, and the induced field reinforces the applied field resulting in an average local field $\simeq 2.2$ times the applied field strength. The largest induced fields are in the xy plane which is reasonable, as 9 out of 13 valence electron pairs lie approximately in this plane. Bare polarizability matrices, obtained using average local fields, $\mathcal{E}$, in (4), are given for the same electron pairs in table 4. The matrices are now nearly symmetric, with the remaining inequality in off-diagonal elements probably a result of averaging the local field over the bond. Clearly the bare matrices are much closer to satisfying Onsager's principle, with the corollary of improved transferability, than are the dressed matrices.

Calculation of the hyperpolarizability matrices is done in a similar way. Dressed

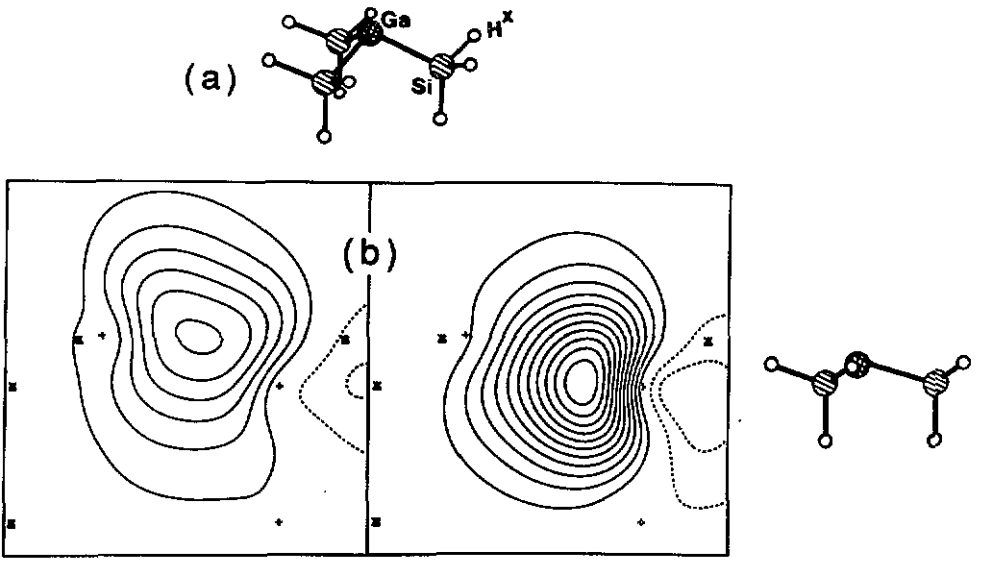

Figure 4. A schematic diagram (*a*) of the $Si_3GaH_9^x$ cluster and contour plots of (*b*) the Si–Ga bond GVB orbitals. Contour intervals are 0.02 au.

Table 4. Bare polarizabilities for (*a*) Si–As and (*b*) Si–Ga bonds in bond coordinates, and (*c*) the As lone pair in surface coordinates, in units of 10^{-30} m^3.

(*a*)	⊥	⊥′	∥	(*b*)	⊥	⊥′	∥	(*c*)	*x*	*y*	*z*
⊥	6.1	0.0	0.7	⊥	11.5	0.0	5.0	*x*	14.4	0.0	0.0
⊥′	0.0	7.1	0.0	⊥′	0.0	11.4	0.0	*y*	0.0	13.6	0.0
∥	−0.4	0.0	15.0	∥	2.4	0.0	16.8	*z*	0.0	0.0	12.0

hyperpolarizabilities are obtained by equating the quadratic polarization of bond orbitals to the hyperpolarizability for particular field directions. When average local fields are used to extract bare bond hyperpolarizabilities in (4), a system of linear equations must be solved that depends parametrically and quadratically on average local fields. A symmetry present in static susceptibilities is therefore used to simplify the extraction of bare hyperpolarizabilities. For an electronic system in the lossless regime, all $\chi^{(2)}_{ijk}$ tensor elements that are related by a rearrangement of the order of the subscripts are equal in magnitude and sign:

$$\chi^{(2)}_{ijk} = \chi^{(2)}_{ikj} = \chi^{(2)}_{kji} \qquad \text{etc.} \tag{7}$$

This is Kleinman's conjecture [33] and tensor elements related in this way obey Kleinman 'symmetry'. A reduced set of linear equations is then solved in which elements related by interchanging the last two indices are equated. This is expected to improve the accuracy of bare hyperpolarizabilities which can only be obtained when fields have been applied in two orthogonal directions. Note that some hyperpolarizabilities, which should be zero by symmetry, are small but non-zero ($\simeq (0.1\text{–}0.2) \times 10^{-40}$ m^4 V^{-1}) through the limitations of numerical accuracy of the method. These have been entered as zeros in the tables so as not to detract from the information being conveyed.

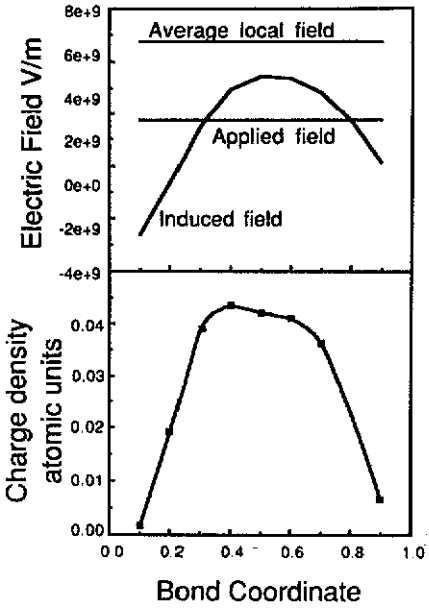

Figure 5. (*a*) Applied field, induced field and average local field resolved in the x direction in a $Si_3AsH_9^+$ cluster when a field is applied in the x direction. (*b*) Charge density of the Si–As bond pair along the Si–As bond axis. Bond coordinates 0.0 and 1.0 correspond to the As and Si nuclei, respectively.

Dressed Si–As and Si–Ga bond matrices and the As lone pair tensor are given in table 5. When the matrices are extracted from the same bond polarization data using the average local field and imposing Kleinman symmetry, the bare hyperpolarizability matrices shown in table 6 are obtained.

Table 5. Dressed hyperpolarizabilities for (*a*) Si–As and (*b*) Si–Ga bond pairs in bond coordinates, and (*c*) the As lone pair in surface coordinates, in units of 10^{-40} m^4 V^{-1}.

(*a*)	$\perp\perp$	$\perp'\perp'$	$\parallel\parallel$	$\perp'\parallel$	$\perp\parallel$	$\perp'\perp$
$\perp$	−0.9	1.3	1.4	0.0	−0.6	0.0
$\perp'$	0.0	0.0	0.0	−0.1	0.0	−0.1
$\parallel$	−5.0	−1.0	12.8	0.0	−1.9	0.0
(*b*)	$\perp\perp$	$\perp'\perp'$	$\parallel\parallel$	$\perp'\parallel$	$\perp\parallel$	$\perp'\perp$
$\perp$	−3.8	3.8	−1.7	0.0	−9.1	0.0
$\perp'$	0.0	0.0	0.0	−0.7	0.0	0.3
$\parallel$	4.1	−0.7	0.6	0.0	9.6	0.0
(*c*)	xx	yy	zz	xy	xx	xy
x	−1.1	1.7	0.0	0.0	−3.8	0.0
y	0.0	0.0	0.0	−3.8	0.0	1.1
z	−5.3	−7.0	−2.8	0.0	0.0	0.0

Bond polarizabilities are not used to calculate a surface dielectric susceptibility, since to how many layers deep such a susceptibility would extend is not well defined. However, it is more reasonable to assume that the second-order polarization is much more localized at the surface. Surface second-order susceptibilities, $\chi^{(2)}$, are calculated by summing over the bond pair and lone pair dressed hyperpolarizabilities for

Table 6. Bare hyperpolarizabilities for (*a*) Si–As and (*b*) Si–Ga bonds in bond coordinates, and (*c*) the As lone pair in surface coordinates, in units of 10^{-40} m^4 V^{-1}.

(*a*)	$\perp\perp$	$\perp'\perp'$	$\parallel\parallel$	$\perp'\parallel$	$\perp\parallel$	$\perp'\perp$
$\perp$	−0.6	1.0	0.2	0.0	−0.6	0.0
$\perp'$	0.0	0.0	0.0	−0.7	0.0	1.0
$\parallel$	−0.6	−0.7	1.3	0.0	0.2	0.0

(*b*)	$\perp\perp$	$\perp'\perp'$	$\parallel\parallel$	$\perp'\parallel$	$\perp\parallel$	$\perp'\perp$
$\perp$	0.2	8.7	−0.7	0.0	−1.5	0.0
$\perp'$	0.0	0.0	0.0	−1.4	0.0	8.7
$\parallel$	−1.5	−1.4	1.1	0.0	−0.7	0.0

(*c*)	xx	yy	zz	xy	zx	xy
x	−0.7	0.9	0.0	0.0	−3.4	0.0
y	0.0	0.0	0.0	−3.9	0.0	0.9
z	−3.4	−3.9	−2.7	0.0	0.0	0.0

both surfaces. Surface $\chi^{(2)}$ matrices, the sum of bond hyperpolarizability per unit surface area, are given in table 7 in m^2 V^{-1}.

Table 7. Surface $\chi^{(2)}$ matrices for (*a*) Si_3As and (*b*) Si_3Ga bilayers, in units of 10^{-21} m^2 V^{-1}.

(*a*)	xx	yy	zz	xy	zx	xy	(*b*)	xx	yy	zz	xy	zx	xy
x	3.7	−3.7	0.0	0.0	−2.3	0.0		2.7	−2.6	0.0	0.0	8.6	0.0
y	0.0	0.0	0.0	−2.6	0.0	−3.7		0.0	0.0	0.0	11.0	0.0	−1.1
z	−5.6	−5.1	1.7	0.0	0.0	0.0		−2.3	−2.5	3.4	0.0	0.0	0.0

6. Discussion

The sources of linear and non-linear polarization at surfaces can be analysed more easily in a bond framework than the conventional band framework. The bare matrices are the appropriate quantities in discussing the bond response and the dressed quantities are the relevant ones for the response of the whole system.

Table 1 shows static polarizabilities and hyperpolarizabilities for the hydrogen molecule for several basis sets at the Hartree–Fock level. Theoretical studies of these quantities for the hydrogen molecule, which incorporate electron correlation, have shown that this is much less important than an adequate basis set in obtaining accurate calculated values [34]. This is borne out by table 1 since good agreement with both experiment, and extended basis set calculations that incorporate electron correlation, is obtained using a double-ζ valence plus double-ζ polarization basis set. Molecular hydrogen is the only molecule that contains an 'isolated' chemical bond: all other molecules contain more than one electron pair which mutually polarize each other via fields induced in the presence of an applied field. This is contained in the dressed polarizabilities of table 3, but the bare polarizabilities of table 4 represent

the polarizability of a bond in the absence of mutual polarization. For the Si–As bond, the bare $\alpha'_{\perp\perp}$, $\alpha'_{\perp'\perp'}$ and $\alpha'_{\parallel\parallel}$ components are 6.1, 7.1 and 15.0×10^{-30} m^3, respectively, compared with 8.4, 8.4 and 11.9×10^{-30} m^3 for H–H. The diagonal elements of polarizability of the Si–Ga bond are similar in magnitude to those of the Si–As bond, except for somewhat larger $\alpha'_{\perp\perp}$ and $\alpha'_{\perp'\perp'}$ components. The bare polarizabilities for the surface bond pairs are similar in magnitude to those of the hydrogen molecule, and these are enhanced by the local field in the surface or cluster to give larger dressed polarizabilities. The off-diagonal elements of the bare polarizability matrix ought to be zero if the bond charge density has a 'cigar shape' and the major polarizability matrix axis lies along the cigar axis. From table 4(*a*) it can be seen that this is so for the Si–As bond. Inspection of the Si–As bond orbital amplitudes in figure 3 shows that the bond charge density has approximately this cylindrical symmetry. In contrast, the Si–Ga bond polarizability matrix (table 4(*b*)) has non-zero off-diagonal elements when the bond coordinate system of axes is used. The off-diagonal elements are much reduced, however, when the axes are rotated to surface coordinates. This is reflected in the orbital character of the Si–Ga bond in the GVB wave function and is a result of strain in this surface structure. The bond lobe localized on the Si atom is comparable to the equivalent lobe in a Si–Si bond or the Si–As bond, but the lobe localized on the Ga atom is unusual. It extends from the Ga atom nearly parallel to the surface. This bond is bent because the Ga atom cannot form three ideal 'sp^2-hybridized' bonds to silicon—the positions of Si atoms in the Si(111) surface constrain the geometry that the Si–Ga bonds can attain, resulting in Si–Ga bonds significantly shorter than the sum of the Si and Ga covalent radii but with their charge density bent outwards from the surface. The bare bond polarizability matrix consequently has non-zero off-diagonal elements in bond coordinates. The bent charge density profile of the Si–Ga bond also has consequences in the bond hyperpolarizability tensor.

In table 2 first hyperpolarizabilities for a modified, acentric H_2 molecule were presented. The cylindrical symmetry of the molecule requires that $\beta_{\parallel\perp\perp} = \beta_{\parallel\perp'\perp'}$. From Kleinman symmetry, $\beta_{\parallel\perp\perp} = \beta_{\perp\parallel\perp}$ and $\beta_{\parallel\perp'\perp'} = \beta_{\perp'\parallel\perp'}$ and so *all* these elements are equal. $\beta_{\parallel\parallel\parallel}$ is the other unique element: it corresponds to the hyperpolarizability parallel to the bond axis, with a field applied parallel to that axis. It has the same sign as the other elements and is four times larger. So, for the simplest, hypothetical acentric chemical bond a combination of symmetry requirements and Kleinman symmetry lead to only *two* unique elements in the bond first hyperpolarizability tensor, with the tensor being dominated by the $\beta_{\parallel\parallel\parallel}$ element.

Turning to the more complex systems, dressed hyperpolarizabilities, in bond coordinates, for the Si–As and Si–Ga bonds were given in table 5, along with dressed hyperpolarizabilities for the As lone pair in surface coordinates. $\beta_{\parallel\parallel\parallel}$ is the dominant element for the Si–As bond, as is the case in the modified H–H molecule. The dressed Si–As hyperpolarizability matrix has the correct symmetry for a bond with a single mirror plane (appendix B). Likewise, the Si–Ga bond and As lone pair matrices satisfy the symmetry requirements for a bond with a single mirror plane, and a pair with $3m$ point group symmetry, respectively. However, deviations in magnitude occur for elements of the lone pair matrix which ought to be equal. The dressed lone pair and bond pair matrices do not conform perfectly to Kleinman symmetry. Imperfect conformation of dressed hyperpolarizability matrices to Kleinman symmetry is a result of separating the whole cluster into pieces and is not because of limited accuracy of

the method; the whole cluster conforms very well to Kleinman symmetry in a static field.

More may be learnt about the non-linear properties of the bond from the bare hyperpolarizabilities than the dressed versions, as was the case for polarizabilities, but it should be recalled that the bare hyperpolarizabilities are extracted with the constraint that they obey Kleinman symmetry. From table 6(*a*) it can be seen that the element $\beta'_{\parallel\parallel\parallel}$ is still the largest for the Si–As bond, but it is not dominant. (Recall that in section 2, bare and dressed quantities were distinguished by adding a prime in the latter case.) In addition to elements that produce a non-linear polarization parallel to the bond axis, there are also elements that produce a non-linear polarization along the $\perp'$ axis, perpendicular to the bond. For a bond of perfect cylindrical symmetry, all elements, except $\beta'_{\perp\perp\parallel}$ and $\beta'_{\perp'\perp'\parallel}$, responsible for non-linear polarization perpendicular to the bond are zero, but the charge density in the Si–As bond is slightly bent *inwards* [20], so there is a non-zero $\beta'_{\perp\perp'\perp'}$ element: a field parallel to the solid surface but perpendicular to the bond (along $\perp'$) will produce a non-linear polarization in the $\perp$ direction, outwards from the surface but perpendicular to the bond. Elements of the dressed hyperpolarizability matrices are quite different in magnitude and, sometimes, in sign, but the bare matrix elements of the Si–As and Si–Ga bonds are similar! The $\beta'_{\parallel\parallel\parallel}$ elements are comparable for both Si–As and Si–Ga bonds in magnitude and sign. The $\beta'_{\parallel\perp\perp}$ and $\beta'_{\parallel\perp'\perp'}$ elements for either bond are approximately equal (as they ought to be for a cylindrical acentric bond (appendix B)) but differ in magnitude between bonds by a factor of 2, the Si–Ga bond giving the larger response. The $\beta'_{\perp\perp'\perp'}$ element has a value of 1.0×10^{-40} m^4 V^{-1} for the Si–As bond. The same element has a much larger value of 8.7×10^{-40} m^4 V^{-1} for the Si–Ga bond, and is the dominant element in the bare matrix. This is another consequence of the highly non-cylindrical charge distribution of the Si–Ga bond, mentioned earlier in this section. Recall that this element is *zero by symmetry* for a perfectly cylindrical bond. This element is also relatively large in the dressed matrices, so the large values in the bare matrices are not an artifact of the way in which these matrices are extracted. It is clear that, for bonds in lowered symmetry situations such as surfaces, a bond hyperpolarizability can depend strongly on its environment [35]. Matrix elements which become non-zero through symmetry lowering can actually dominate the non-linear response, in contrast to the response of the acentric bond with perfect cylindrical symmetry (modified H_2 molecule) for which the $\beta_{\parallel\parallel\parallel}$ element is the largest.

The bare hyperpolarizability matrix for the lone pair has $3m$ point group symmetry. Its largest elements (in surface coordinates) are β'_{zxx} and β'_{zyy}: when a field is applied perpendicular to the lone pair symmetry axis, the lone pair z expectation value is reduced as it polarizes along x or y directions. There is no linear α_{zx} or α_{zy} lone pair polarizability by symmetry, so all such polarization is non-linear. The β'_{zzz} component is the other major component of lone pair hyperpolarizability.

The non-linear polarization can cancel or reinforce between different pairs and it is the sum of all pairs that gives the overall non-linear response. The surface $\chi^{(2)}$ matrices, which are obtained when bond pair and lone pair hyperpolarizabilities are summed in surface coordinates, are now described. The surface non-linear susceptibility is the hyperpolarizability per unit surface area, and it is this quantity that may be compared to SHG experiment. For a homogeneous surface one would expect the greatest component in $\chi^{(2)}$ to be $\chi^{(2)}_{zzz}$, because it is along the z direction, perpendicular to the surface, that inversion symmetry is broken. This has been

assumed in recent models of SHG at surfaces of nearly-free-electron metals [36] and semiconductors [14]. In 'structured' surfaces, such as semiconductor surfaces with valence charge localized in directional bonds, this is not the case as demonstrated by the results given above. For the Si(111) 1 × 1 As surface, cluster models predict that the largest elements are $\chi^{(2)}_{xxx}$ and $\chi^{(2)}_{xyy}$. They have major contributions from the $\beta_{\parallel\parallel\parallel}$ and $\beta_{\perp\perp'\perp'}$ elements of the dressed bonds. The $\chi^{(2)}_{xxx}$ and $\chi^{(2)}_{xyy}$ elements have their major contribution from the $\beta_{\parallel\parallel\parallel}$ element of the dressed bonds. The $\chi^{(2)}_{zzz}$ element is small because of near cancellation of the lone pair and bond pair non-linear responses. The Si(111) 1 × 1 As surface $\chi^{(2)}$ matrix obeys $3m$ point group symmetry well, but elements which ought to be identical by Kleinman symmetry, differ by a factor of 2. This arises because the twelve Si–H^x cluster-terminating bond pairs have been separated from the Si–As bond pairs and the As lone pair.

For the Si(111) 1 × 1 Ga surface there is a similar pattern to that for the As-terminated surface. The $\chi^{(2)}_{xxx}$, $\chi^{(2)}_{xyy}$, $\chi^{(2)}_{zxx}$ and $\chi^{(2)}_{zyy}$ elements are all smaller than in the As-terminated surface but the $\chi^{(2)}_{zzz}$ element is larger by a factor of two. This is reasonable because the cancellation between the lone pair and bond pairs in the As-terminated surface is absent in the Ga-terminated surface. A disturbing feature of this $\chi^{(2)}$ is gross violation of Kleinman symmetry: $\chi^{(2)}_{zxx}$ and $\chi^{(2)}_{xzx}$, and $\chi^{(2)}_{zyy}$ and $\chi^{(2)}_{yzy}$ differ in magnitude by factors of $\simeq 4$ and are opposite in sign whereas they should be identical in order for Kleinman symmetry to hold. Again, this arises because the twelve Si–H^x cluster-terminating bond pairs have been separated from the central electron pairs.

The theoretical values presented in table 7 may be compared to experimental values for Si surfaces, either clean or with adsorbed As. Absolute measurements [15] of the SHG intensity have found responses in the range $(2\text{–}7)\times 10^{-21}$ m^2 V^{-1} in good agreement with the values reported in table 7.

7. Summary and conclusions

Polarizabilities and hyperpolarizabilities of bonds in two semiconductor surfaces have been extracted from induced dipoles of localized GVB bond orbitals in static applied fields. If the field acting on each bond pair is assumed to be the applied field, dressed matrices are extracted that violate Onsager's principle, and do not reflect the symmetry of the GVB orbitals. On the other hand, if the fields that are generated by each polarized bond are combined along with the applied field to produce an average local field, the polarizability matrices satisfy Onsager's principle much better and the hyperpolarizability matrices have the symmetry of the GVB orbitals. 'Bare' hyperpolarizability matrices extracted in this way are analysed as sources of non-linear polarization in each of the surfaces studied. In general, the $\beta'_{\parallel\parallel\parallel}$ matrix element of an acentric, cylindrical bond pair is dominant, but in situations where the cylindrical symmetry of a bond pair is broken (the bond is 'bent'), such as in surface structures, other matrix elements that are otherwise zero by symmetry may become large and may dominate the hyperpolarizability matrix. Surface non-linear susceptibilities may be generated from dressed bond hyperpolarizabilities by summing over the bond pairs in a representative cluster. Unlike in the case of an electronically homogeneous (metallic) surface, the largest surface $\chi^{(2)}$ element of a semiconductor surface is not necessarily $\chi^{(2)}_{zzz}$. For the Si(111) 1 × 1 As surface the order of inequivalent

elements is $\chi^{(2)}_{xxx} > \chi^{(2)}_{xxz} > \chi^{(2)}_{zzz}$ while for the Si(111) 1 × 1 Ga surface the order of inequivalent elements is $\chi^{(2)}_{zzz} > \chi^{(2)}_{xxz} > \chi^{(2)}_{xxx}$ (neglecting anomalous $\chi^{(2)}_{yzy}$ and $\chi^{(2)}_{xzx}$ elements).

Cluster methods for obtaining non-linear susceptibilities of solids are an attractive alternative to band-structure methods. They are computationally efficient, and in the case of systems with very large unit cells they may present the only practicable means of calculating the non-linear electric susceptibility.

Acknowledgments

This work was supported by the Commission of the European Communities program ESPRIT, basic research action No 3177; 'EPIOPTICS' and SCIENCE, twinning contract No SC1-0001-C-(EDB). The authors are grateful to R Del Sole for helpful discussions and to R P Messmer who suggested the idea of cluster calculations of optical response.

Appendix A. Definitions of units and local fields

SI units have been used throughout. Bulk polarization is in C m^{-2}. For a bond it is not possible to give a polarization per unit volume since the 'volume' of the bond is not well defined. Hence bond-induced dipoles are in units of C m and the bond polarizability and first hyperpolarizability are in units of m^3 and m^4 V^{-1}, respectively. The bulk second-order susceptibility in these units is m V^{-1} while the surface second-order susceptibility is in m^2 V^{-1}.

The local field that we use to extract bare parameters for bonds is the same as the local field acting on an ion in Ashcroft and Mermin's 'theory of the local field' [37]. This is, 'the microscopic field at the position of the ion [bond], diminished by the contribution to the microscopic field from the ion [bond] itself'. The microscopic electric field, $e(x,t)$, in a solid is the field, rapidly varying in time and space, produced by the instantaneous positions of the electrons and nuclei. The *macroscopic* electric field, $\boldsymbol{E}(x,t)$, appearing in the macroscopic Maxwell's equations is the *spatially averaged* microscopic field [38]. This local field differs from another 'local field effect' frequently encountered in discussions of the dielectric response of semiconductors and insulators [39]. There, the contributions of off-diagonal elements in the inverse dielectric function, which relates the potential seen by a test charge to an applied potential (equation (A1)),

$$V_{\text{test}}(q',\omega) = \epsilon^{-1}(q',q;\omega)\, V_{\text{app}}(q,\omega) \tag{A1}$$

are attributed to 'local field effects'.

Appendix B. Symmetries in bond parameter matrices and surface susceptibilities

The linear induced dipole, $p^{(1)}$, of a cluster may be expressed as a sum over bonds via

$$p^{(1)} = \sum_n p_n^{(1)} = \sum_n \alpha_n E \tag{B1}$$

where $p_n^{(1)}$ is the linear induced dipole of the nth bond, α_n is the dressed polarizability matrix of the nth bond and E is the applied field. The α_n matrices differ by bond type and by bond orientation; only when bond type and bond orientation coincide will the polarizability matrix be the same. The induced dipole of each bond is

$$p_{n,i}^{(1)} = \alpha_{n,ij} E_j. \tag{B2}$$

For an isolated body, Onsager's principle [31] requires that the matrix with element $\alpha_{n,ij}$ be symmetric (equation (6)). The shapes of GVB bond pairs (combined pairs of GVB bond orbitals) shown in figures 3 and 4 are ellipsoidal, the principal axes lying along, and perpendicular to, the bond axis. Because of the almost symmetrical charge distribution of a bond pair about these axes, the axes of the representation quadric of the bare bond matrix [40] are expected to coincide with the bond axes.

The quadratic induced dipole of a cluster, $p^{(2)}$, may also be expressed as a sum over bonds:

$$p^{(2)} = \sum_n p_n^{(2)} = \sum_n \beta_n E^2 \tag{B3}$$

where $p_n^{(2)}$ is the quadratic, dressed polarization of the nth bond, β_n is a third-rank tensor for the nth bond and E is the applied field. The quadratic induced dipole of each bond is given by

$$p_{n,i}^{(2)} = \beta_{n,ijk} E_j E_k. \tag{B4}$$

Since no physical significance can be attached to an exchange of E_j and E_k, $\beta_{ijk} = \beta_{ikj}$, the tensor can be reduced to a 3×6 matrix, d_{ij}, so the vector components of $p_n^{(2)}$ are given [41] by

$$\begin{pmatrix} p_x \\ p_y \\ p_z \end{pmatrix} = \begin{pmatrix} d_{11} d_{12} d_{13} d_{14} d_{15} d_{16} \\ d_{21} d_{22} d_{23} d_{24} d_{25} d_{26} \\ d_{31} d_{32} d_{33} d_{34} d_{35} d_{36} \end{pmatrix} \begin{pmatrix} E_x^2 \\ E_y^2 \\ E_z^2 \\ 2E_y E_z \\ 2E_x E_z \\ 2E_x E_y \end{pmatrix} \tag{B5}$$

where the subscripts jk have been replaced by a single symbol: $\perp\perp$ or $xx \equiv 1$; $\perp'\perp'$ or $yy \equiv 2$; $\|\|$ or $zz \equiv 3$; $\perp'\| \equiv \|\perp' \equiv 4$ or $yz \equiv zy \equiv 4$; $\perp'\| \equiv \|\perp' \equiv 5$ or $xz \equiv zx \equiv 5$; $\perp'\perp \equiv \perp\perp' \equiv 6$ or $xy \equiv yx \equiv 6$. The non-linear susceptibility matrices given in tables 2, and 5 to 7 are d_{ij} matrices of this form. Apart from Kleinman symmetry, there are symmetries imposed on the d_{ij} matrix by the point group of the cluster or solid surface. Matrix symmetries for the non-linear response of clusters with $3m$ point group symmetry and individual bond pairs with m point group symmetry are given below in a standard notation to be described. Large dots indicate non-zero elements, small dots are elements which are zero by symmetry. Dots that are joined by continuous lines are elements which are equal in magnitude; two dots joined in this way that are filled and unfilled are elements opposite in sign; if they are both filled or unfilled they have the same sign.

The clusters studied (and surfaces that they represent) have $3m$ point group symmetry. The d_{ij} matrix for the response of the entire cluster or the surface ought to have the symmetries:

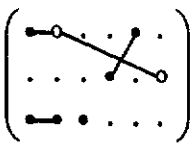

(B6)

Each of the clusters possesses $3m$ symmetry, as do their *total* wave functions (products of spatial orbitals and spin functions), but each of the bond pairs is required to possess only a single mirror plane (m symmetry). In this case the symmetries of the d_{ij} matrix are

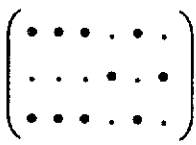

(B7)

i.e. no non-zero elements are necessarily equal. Provided that the d_{ij} matrix is in bond coordinates, if the bond is not bent, it will possess two mirror planes, perpendicular to one another, that lie along the bond axis, and the d_{ij} matrix will have $4mm$ point group symmetry. In this case a bond hyperpolarizability can be described by three unique elements only (compare the asymmetric hydrogen molecule in table 2):

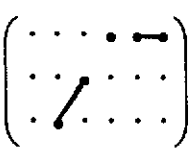

(B8)

Appendix C. Details of computations and basis sets

All GVB computations [30] were performed using the GAMESS program [42]. The core states of the heavy atoms were replaced by effective-core potentials (ECP) which closely reproduce the all-electron (AE) ground state properties of similar systems to these clusters [10]. This was checked for the systems studied here by computing AE

and ECP bond polarizabilities of the Si–Si bond. The polarizabilities and induced fields found in AE and ECP calculations, with similar valence double-ζ-plus-polarization basis sets appropriate for each core type, were compared for the Si–Si bond in a $Si_2H_6^x$ cluster. Bare polarizabilities of AE and ECP calculations differed by 6%; induced fields in the region where bond charge density was concentrated were similar. The ECP basis sets for Si [43], As [44] and Ga [44] were the 2s2p bases developed for their respective ECPs [43, 44] supplemented by a single-ζ d polarization function on each heavy atom ($\zeta_{Si} = 0.032$, $\zeta_{As} = 0.035$, $\zeta_{Ga} = 0.035$). The AE basis set for Si was the 11s7p basis of Huzinaga [45] contracted to 6s4p [46]. The modified hydrogen basis, H^x, used to terminate the clusters was the single-ζ basis of Schultz and Messmer [27].

References

[1] Levine B F 1973 *Phys. Rev.* B **7** 2600; 1969 *Phys. Rev. Lett.* **22** 787; 1970 *Phys. Rev. Lett.* **25** 440; 1974 *Phys. Rev. Lett.* **33** 368

[2] Jha S S and Bloembergen N 1968 *Phys. Rev.* **171** 891

[3] Flytzanis Ch and Ducuing J 1969 *Phys. Rev.* **178** 1218

[4] Aspnes D E 1972 *Phys. Rev.* B **6** 4648

[5] Fong C Y and Shen Y R 1975 *Phys. Rev.* B **12** 2325

[6] Ghahramani E, Moss D J and Sipe J E 1991 *Phys. Rev.* B **43** 8990

[7] Miller CK, Orr B J and Ward J F 1977 *J. Chem. Phys.* **67** 2109; 1981 *J. Chem. Phys.* **74** 4858

[8] Messmer R P and Schultz P A 1986 *Phys. Rev. Lett.* **57** 2653
Schultz P A and Messmer R P 1987 *Phys. Rev. Lett.* **58** 2416

[9] Patterson C H and Messmer R P 1990 *J. Am. Chem. Soc.* **112** 4138

[10] Patterson C H and Messmer R P 1990 *Phys. Rev.* B **42** 7530

[11] McGilp J F 1990 *J. Phys.: Condens. Matter* **2** 7985

[12] Shen Y R 1985 *J. Vac. Sci. Technol.* B **3** 1464

[13] Mizrahi V and Sipe J E 1987 *J. Opt. Soc. Am.* B **5** 660

[14] Cini M 1991 *Phys. Rev.* B **43** 4792

[15] Kelly P V, Tang Z R, Woolf D A, Williams R H, McGilp J F 1991 *Surf. Sci.* **251–2** 87
Kelly P V, O'Mahony J D, McGilp J F and Rasing Th 1992 *Appl. Surf. Sci.* at press

[16] Wilhelm H, Richter W, Rossow U, Zahn D R T, Woolf D A, Westwood D I and Williams R H 1991 *Surf. Sci.* **251–2** 556

[17] Reining L, Cini M and Del Sole R 1992 work in progress

[18] Olmstead M A, Bringans R D, Uhrberg R I G and Bachrach R Z 1986 *Phys. Rev.* B **34** 6041
Uhrberg R I G, Bringans R D, Olmstead M A, Bachrach R Z and Northrup J E 1986 *Phys. Rev.* B **35** 3945

[19] Becker R S, Swartzenruber B S, Vickers J S, Hybertsen M S and Louie S G 1988 *Phys. Rev. Lett.* **60** 116

[20] Patterson C H and Messmer R P 1989 *Phys. Rev.* B **39** 1372

[21] Morse D C and Mele E J 1989 *Phys. Rev.* B **40** 3465

[22] Patel J R, Golovchenko J A, Freeland P E and Gossmann H-J 1987 *Phys. Rev.* B **36** 7715

[23] Headrick R L and Graham W R 1988 *Phys. Rev.* B **37** 1051
Copel M, Tromp R M and Koehler U K 1988 *Phys. Rev.* B **37** 10756

[24] Zegenhagen J E, Hybertsen M S, Freeland P E and Patel J R 1988 *Phys. Rev.* B **38** 7885

[25] Chen D M, Golovchenko J A, Bedrossian P and Mortensen K 1988 *Phys. Rev. Lett.* **61** 2867

[26] Redondo A, Goddard W A III, Swarts C A and McGill T C 1981 *J. Vac. Sci. Technol.* **19** 498; 1982 *J. Vac. Sci. Technol.* **21** 344

[27] Schultz P A and Messmer R P 1986 *Phys. Rev.* B **34** 2532

[28] Amore-Bonapaste A, Lapiccirella A, Tomassini N and Capizzi M 1987 *Phys. Rev.* B **36** 6228; 1989 *Phys. Rev.* B **39** 12 630

[29] Fedders P A and Carlsson A E 1989 *Phys. Rev.* B **39** 1134

[30] Hurley A C, Lennard-Jones J E and Pople J A 1953 *Proc. R. Soc.* A **220** 446
Hay P J, Hunt W J and Goddard W A III 1972 *J. Am. Chem. Soc.* **94** 8293

Bobrowicz F W and Goddard W A III 1977 *Modern Theoretical Chemistry* vol 3, ed H F Schaefer III (New York: Plenum) ch 4
[31] Herrendörfer D, Weaire D, McGilp J F and Patterson C H 1992 work in progress
[32] See, for example, Nye J F 1967 *Physical Properties of Crystals* (Oxford: Clarendon) pp 207ff
[33] Kleinman D A 1962 *Phys. Rev.* **126** 1977
[34] Berns R M and Wormer P E S 1981 *Mol. Phys.* **44** 1215
Bishop D M and Pipin J 1987 *Phys. Rev.* A **36** 2171
[35] This does not necessarily mean that values of bond parameters are irreproducible for a particular bond type. The Si–Ga bond in the Si(111) surface is a special case of a highly strained bond.
[36] Chizmeshya A and Zaremba E 1988 *Phys. Rev.* B **37** 2805
Liebsch A and Schaich W L 1989 *Phys. Rev.* B **40** 5401
Ishida H and Liebsch A 1991 *Phys. Rev.* B **42** 5505
[37] Ashcroft N W and Mermin N D 1976 *Solid State Physics* (Philadelphia, PA: Holt–Saunders) pp 539ff
[38] Jackson J D 1975 *Classical Electrodynamics* 2nd edn (New York: Wiley) section 6.7
[39] Hanke W and Sham L J 1975 *Phys. Rev.* B **12** 4501
[40] Lovett D R 1989 *Tensor Properties of Crystals* (Bristol: Adam Hilger)
[41] Yariv A 1989 *Quantum Electronics* 3rd edn (New York: Wiley) pp 378ff
[42] Westbrook J D, Blair J T and Krogh-Jespersen K (Rutgers University, NJ): version of the original GAMESS program, developed by Dupuis M, Spangler D, Wendolowski J, Elbert S and Schmidt M 1980 *GAMESS program* National Resource for Computation in Chemistry Software Catalog, vol 1, Program QG01 (Lawrence Berkeley Laboratory, United States Department of Energy)
[43] Rappé A K, Smedley T A and Goddard W A III 1981 *J. Phys. Chem.* **85** 1662
[44] Wadt W R and Hay P J 1982 *J. Chem. Phys.* **57** 738
[45] Huzinaga S 1971 *Report* Department of Chemistry, University of Alberta, Canada (unpublished)
[46] Dunning T H Jr and Hay P J 1977 *Modern Theoretical Chemistry* vol 4 (New York: Plenum) p 1
[47] Bishop D M and Pipin J 1987 *Phys. Rev.* A **36** 2171
[48] Mizrahi V and Shelton D P 1985 *Phys. Rev.* A **32** 3454